Advances in Redox Research 9 (2023) 100083

Contents lists available at ScienceDirect

Advances in Redox Research

journal homepage: www.elsevier.com/locate/arres

Full Length Article

Peroxiredoxin-1 is an H_2O_2 safe-guard antioxidant and signalling enzyme in M1 macrophages

Daria Ezeriņa [a,b,c,+], Trung Nghia Vo [a,b,c,+], Ting Luo [a,b,c,+], Yvon Elkrim [d,e], Anna Escoda Suarez [a,b,c], Gaëtan Herinckx [f], Didier Vertommen [f], Damya Laoui [d,g], Jo A. Van Ginderachter [d,e,*], Joris Messens [a,b,c,*]

[a] VIB-VUB Center for Structural Biology, Vlaams Instituut Voor Biotechnologie, Brussels B-1050, Belgium
[b] Brussels Center for Redox Biology, Vrije Universiteit Brussel, Brussels B-1050, Belgium
[c] Structural Biology Brussels, Vrije Universiteit Brussel, Brussels B-1050, Belgium
[d] Laboratory of Cellular and Molecular Immunology, Vrije Universiteit Brussel, Brussels B-1050, Belgium
[e] Myeloid Cell Immunology Lab, VIB Center for Inflammation Research, Pleinlaan 2, Brussels B-1050, Belgium
[f] de Duve Institute, MASSPROT platform, UCLouvain, Brussels 1200, Belgium
[g] Laboratory of Dendritic Cell Biology and Cancer Immunotherapy, VIB Center for Inflammation Research, Pleinlaan 2, Brussels B-1050, Belgium

ARTICLE INFO

Keywords:
Peroxiredoxins
Peroxiredoxin-1
M1 macrophages
M2 macrophages
ASK1
ROS

ABSTRACT

Macrophages are characterised by their high plasticity and ability to adapt their phenotype and functionality in response to environmental cues, resulting in a spectrum of activation states the two extremes of which are M1 and M2. Reactive oxygen species, such as hydrogen peroxide, are among the cues that impact macrophage polarisation. Moreover, high levels of hydrogen peroxide play a role in the phagocytic response executed by M1 macrophages. Therefore, macrophages must balance the need to shield themselves from the harmful effects of hydrogen peroxide bursts with the ability to interpret hydrogen peroxide signals from the surroundings and initiate a cellular response. Peroxiredoxins (PRDX) are proteins capable of performing both roles. Specifically, PRDX1 and PRDX5 have been demonstrated to safeguard macrophages against reactive oxygen species while also impacting their polarisation status. Previously conducted studies did not differentiate between the polarisation state of macrophages or investigate the signalling events triggered by PRDXs. In this study, we utilised bone marrow-derived murine macrophages polarised to the M1 and M2 states. Our findings revealed that the expression of PRDX1 was significantly higher in M1 macrophages than in M2 and unpolarised macrophages. Moreover, we present evidence that in M1 macrophages, PRDX1 interacts with ASK1, its established interaction partner, and also binds to other proteins that regulate the cellular antioxidant response. Interestingly, we found that pharmacological elevation of hydrogen peroxide levels leads to an increase in PRDX1 expression on the mRNA level, but not in the highly related PRDX2 expression. Taken together, our findings suggest that PRDX1 plays a critical role in macrophage antioxidant defence and redox signalling, and provide scope for exploring redox-signalling proteins as highly sought-after candidates for macrophage repolarisation.

Introduction

Macrophages are cells of the innate immune system whose main function is to fight infections and take care of tissue homoeostasis. They are characterised by a remarkable plasticity, which allows them to adapt their physiology and function in response to various environmental stimuli [1]. In doing so, they can adopt a broad spectrum of activation states or phenotypes, with the extreme ends being M1 (also known as "pro-inflammatory" or "classically activated") and M2 (also referred to as "anti-inflammatory" or "alternatively activated") macrophages [2]. An important example of macrophage plasticity is provided by macrophages present in the tumour microenvironment (TME). The TME is a dynamic microenvironment consisting of vasculature, various immune cells, fibroblasts, and components of the extracellular matrix, which are all regulated by cancer cells through a range of signalling molecules [3]. While M1 can kill cancer cells via the production of various

* Corresponding authors.
E-mail addresses: Jo.Van.Ginderachter@vub.be (J.A. Van Ginderachter), joris.messens@vub.be (J. Messens).
+ These authors contributed equally.

https://doi.org/10.1016/j.arres.2023.100083
Received 11 May 2023; Received in revised form 11 September 2023; Accepted 18 September 2023
Available online 21 September 2023

pro-inflammatory cytokines and reactive oxygen or nitrogen species (ROS and RNS, respectively), M2 cells produce anti-inflammatory cytokines and trophic factors, thereby promoting cancer progression [2]. Hence, tumours benefit from the presence of M2 macrophages in the TME and can even actively polarise macrophages to an M2 phenotype [3], resulting in a gradual accumulation of more M2-orientated macrophages in the TME in function of time [4–6].

A key role in macrophage polarisation to M2 has been attributed to ROS [7,8], and ROS scavengers have been shown to not only prevent M2 polarisation, but also to inhibit tumour progression in a colorectal cancer model [9]. However, there is also evidence to suggest the opposite, that ROS actually promote M1 polarisation [10,11]. Aside from an effect on polarisation and tumour-killing by M1 macrophages, TAM-produced ROS have also been reported to regulate the onset of TAM apoptosis, which eventually leads to tumour regression [12], as well as to promote the adherence of circulating cancer cells during the metastatic cascade [13]. Taken together, ROS seem to play a multifaceted role in macrophages of the TME, which is most likely determined by a combination of various factors, such as tumour stage at the cellular level, and the nature and concentration of the ROS at the molecular level. Of note, ROS is understood as a collective term for species of varying reactivities and lifetimes in the cell. The most likely signalling function performed by ROS is through hydrogen peroxide (H_2O_2), which has a longer lifetime within the cell [14].

To control ROS levels and to coordinate the cellular response to ROS, macrophages must possess a mechanism that allows them to detect ROS, keep their levels under control and be able to convert a ROS signal to a cellular response. The obvious candidate proteins for sensing intracellular ROS are peroxiredoxins (Prdxs). Mammals possess a family of six Prdx isoforms that are capable of reducing H_2O_2, lipid peroxides, and peroxynitrite, though structural and kinetic studies have shown H_2O_2 to be the preferential substrate [15,16]. These isoforms are abundantly expressed and can be found in various organelles within the cell, depending on the specific isoform [17]. Mechanistically, at least for the typical cytosolic 2-Cys-Prdxs, Prdx1 and Prdx2, peroxide reduction happens through the formation of sulphenic acid (Cys-OH) on the peroxidatic cysteine of Prdx (Cys_p). This sulphenic acid is subsequently attacked by the resolving cysteine (Cys_R) of another subunit, resulting in the formation of an intermolecular disulphide bond and Prdx dimerisation [18]. This disulphide bond is subsequently reduced by the thioredoxin system at the expense of NADPH [19]. At the same time, Prdxs can engage in redox relays with other proteins, either at the sulphenic acid stage or at the Cys_p-Cys_R disulphide stage, through a nucleophilic attack by a target protein. Though there is evidence that all six Prdx mammalian isoforms engage in redox relays with a multitude of target proteins [20], only two have been explored in mechanistic detail: the interaction of Prdx1 with the kinase ASK1 [21,22] and Prdx2 with the transcription factor STAT3 [23,24].

Interestingly, there is evidence of different members of the Prdx family playing roles in macrophages. For example, PRDX1 has been shown to be strongly expressed in murine macrophages compared to other PRDXs, where it is critical for the regulation of H_2O_2 levels [25]. This finding was in line with earlier observations of PRDX1 upregulation upon exposure to H_2O_2 or oxidized low density lipoproteins in peritoneal mouse macrophages and macrophage-derived foam cells, respectively [26,27]. The latter study also demonstrated that upregulated PRDX1 expression also leads to higher p38 phosphorylation, consistent with the activation of ASK1 by PRDX1 [27]. PRDX5, which is atypical and localizes in both the cytoplasm and mitochondria, has been identified as a crucial factor in macrophage polarisation. In the absence of Prdx5, macrophages tend to polarise towards the M2 phenotype via a ROS-dependent mechanism [28].

Although some evidence exists of Prdxs playing a role in macrophages, a comprehensive study on the collective roles of Prdxs in macrophages, especially in relation to their polarisation state, is lacking. In this study, we address this knowledge gap by assessing the expression levels and functional roles of PRDXs in bone marrow-derived murine macrophages polarised to the opposite ends of the polarisation spectrum (M1 and M2) as well as unpolarised (M0) macrophages.

Materials and methods

Mouse strains

Female 6–8 week old C57BI/6J mice were purchased from Janvier. All procedures were conducted following the guidelines of the Belgian Council for Laboratory Animal Science and were approved by the Ethical Committee for Animal Experiments of Vrije Universiteit Brussel (licenses 15–220–8, 18–220–18, and 20–220–36).

Generation and polarisation of mouse bone marrow-derived macrophages (BMDMs)

Bone marrow cells were isolated from tibia and femur and were cultured for 13 days in RPMI- 1640 medium supplemented with 300 μg/mL L-glutamine, 100 mg/mL streptomycin (ThermoFisher Scientific), 100 units/mL penicillin, 20 % (v/v) heat-inactivated FBS (Capricorn Scientific) and 30 % L929-conditioned medium. Then, plastic-adherent bone marrow-derived macrophages (BMDMs) were harvested and seeded at a concentration of 10^6 cells/mL in RPMI-based complete medium. After 1 h of re-adherence, BMDMs were stimulated for 24 h with either a mixture of 100 ng/mL lipopolysaccharide (LPS) from *Escherichia coli* O55:B5 (Sigma-Aldrich) and 20 ng/mL recombinant mouse interferon gamma (IFN-γ) (BD Biosciences) for the generation of M1, or 20 ng/mL recombinant mouse interleukin-4 (IL-4) (Sigma-Aldrich) for the generation of M2.

Antibodies, chemicals and plasticware

The rabbit anti-PRDX1 and anti-PRDX2 antibodies used in this study were a kind gift from Bernard Knoops (UCL, Belgium) [29]. Other antibodies were mouse anti-ASK1 (ThermoFisher Scientific, MA5-15681), rabbit anti-PARK7 (Proteintech, 11681-1-AP), rabbit anti-GAPDH (Sigma-Aldrich, G9545). For Western blot, all antibodies were diluted 1:1000 in Tris-buffered saline with 0.1 % Tween 20 (TBS-T), except anti-GAPDH, which was diluted 1:5000 and anti-PRDX1 and anti-PRDX2, which were diluted 1:2500 in TBS-T with 1 % milk. The secondary antibodies for Western blot used in this study were goat anti-rabbit (1706515, Bio-Rad, USA) and goat anti-mouse (62-6520, ThermoFisher Scientific), which are horseradish peroxidase conjugated and were used at a dilution of 1:5000, also in TBS-T. The protein ladder used in SDS- PAGE was PageRuler Prestained protein ladder (ThermoFisher Scientific, USA). Chemicals used were: Auranofin (Sigma-Aldrich, Cat.A6733), Trolox (Sigma-Aldrich, Cat.238813), xanthine (Sigma-Aldrich, Cat.X0626) and xanthine oxidase (Sigma-Aldrich, Cat.X4376). Plasticware for cell culture was from Avantor (USA).

Preparation of cell lysates

Cells for qRT-PCR, western blot and the NADPH assay were collected 24 h after the addition of polarisation agents. In the case of treatment with Trolox or auranofin, cells were treated with 80 μM Trolox or 0.8 μM auranofin 24 h after the addition of polarisation agents for an additional 14 h (i.e. for a total of 38 h incubation in medium with polarisation agents). The medium still containing the polarisation factors was removed and the cells were washed with ice-cold PBS and collected by trypsinisation. Following three washes with PBS, the cell suspension was washed with 5 mM ice-cold N-ethylmaleimide (NEM) in PBS in the cold. Cells were then washed three times with ice-cold PBS and lysed with lysis buffer (25 mM Tris–HCl, pH 7.4, 150 mM NaCl, 1 mM EDTA, 1 % NP40, 5 % glycerol supplemented with cOmplete™ EDTA-free Protease Inhibitor Cocktail (Roche)) and the HALT phosphatase inhibitor

cocktail). The lysates were incubated on ice for 30 min with vortexing every 10 min and clarified by centrifuging at 7000 x *g* at 4 °C for 10 min, and the supernatant was collected. A Bradford assay using BSA to make the standard curve was performed to quantify the protein concentration in each sample.

RNA extraction, cDNA preparation and quantitative real-time PCR

RNA was extracted from 10^6 polarized BMDMs using the RNeasy Plus Micro kit (Qiagen). RNA was reverse transcribed using oligo(dT) primers (Invitrogen) and SuperScript II reverse transcriptase (Invitrogen). Quantitative real-time PCR (qRT-PCR) was conducted with the CFX Connect Real-Time PCR Detection System (Bio-Rad), using SYBR Green Supermix (Bio-Rad). The PCR cycling parameters were as follows: 30 s at 94 °C, 30 s at 54 °C, and 45 s at 72 °C for 40 cycles. Gene expression was normalised to the housekeeping gene S12. The primers for the determination of gene expression levels are provided in **Supplementary Table 1**.

Western blot

For all western blots, except for the Prdx2 dimerisation blot, the protein samples were treated with 20 mM DTT at RT for 20 min prior to boiling them at 95 °C in loading dye for 5 min. 40 μg of cell lysate were used per sample. Proteins were separated by SDS-PAGE using a 4–20 % Mini-PROTEAN® TGX™ Precast Gel (Bio-Rad) and transferred to methanol-activated polyvinyl difluoride (PVDF) membranes (Bio-Rad) using a tank transfer system (Bio-Rad) for 1 h at 100 V in Towbin buffer. Membranes were blocked with 5 % milk in TBS-T for 1 h at RT and then incubated with appropriate antibodies at dilutions mentioned above at 4 °C overnight. The next day, the membranes were washed three times for 10 min with TBS-T and then incubated with the secondary antibody for 1 h at RT. After another three 10 min washes in TBS-T, the membranes were visualised using Pierce™ ECL Western Blotting Substrate (ThermoFisher Scientific). Membranes were then stripped with Restore™ PLUS Western Blot Stripping Buffer (ThermoFisher Scientific, Cat. 46430) and re-blotted against GAPDH for normalisation. Each western blot was repeated three times, changing the position of the samples to ensure no bias due to potential differences in transfer efficiency.

Western blot analysis

Blots were analysed using ImageJ. The image was converted to an 8-bit type. A region of interest (ROI) was defined based on the biggest band on the blot and its "mean grey value" was determined. The measurements were subsequently analyzed in MS Excel. The mean grey values determined by Image were first inverted by subtracting them from 255, and then background-corrected. This value was then divided by the value calculated for the loading control (GAPDH) to obtain the normalised value.

H_2O_2 determination by Peroxy Orange 1

Cells were collected at the same time as those harvested for western blot. Cells were stained with 5 μM peroxy orange 1 (Tocris Bioscience, Cat. No. 4944) in PBS by incubating them at 37 °C for 40 min. As a positive control, cells were treated with 100 μM H_2O_2 or vehicle and incubated for an additional 20 min. The cells were then washed and measured by flow cytometry with excitation with the 561 nm laser and a 566 LP filter. Unstained cells were used as a background control. The background values were subtracted and the values obtained for M1 and M2 cells normalised to the M0 values or to the vehicle in the case of the positive control.

NADPH determination

NADPH levels were determined in lysates prepared as described above using the Amplite® Fluorimetric NADPH Assay kit "Red Fluorescence" (AAT Bioquest, Cat. 15262) following the manufacturer's instructions. 500 μg of lysate were used for each sample and the signal was measured by fluorescence with $\lambda_{ex} = 540$ nm and $\lambda_{em} = 590$ nm in a fluorescence plate reader (Molecular Devices).

Proximity ligation assay (PLA)

Prior to seeding, each channel of a μ-Slide VI 0.4 (Ibidi, Cat. 80606) was coated with 30 μL 100 μg/mL Poly-L-lysine (Sigma-Aldrich, Cat. P6282) in PBS for 30 min at RT and then washed three times with 100 μL PBS. 35 μL M0/M1/M2 cell suspension (1×10^6 cells/mL) in RPMI containing the corresponding polarisation-stimulating factors was gently added per channel and incubated for 15 min at 37 °C and 5 % CO2 in the incubator. Then each channel was filled with 120 μL RPMI medium containing the polarisation-stimulating factors and the incubation was continued overnight. The next day prior to cell treatment, the old medium was removed and the channels were washed three times with 120 μL PBS (same wash used below). Cells in each channel were treated with 35 μL DMEM + 10 % FBS medium containing PBS (vehicle), 80 μM Trolox, 8 μM xanthine and 1 mU/mL xanthine oxidase, or 0.8 μM auranofin, for 24 h. After treatment, the medium was removed and the channels were washed. For cell fixation, the channels were filled twice with 35 μL 4 % formaldehyde in PBS (PFA) and incubated for 20 min at RT. For cell permeabilisation, the channels were washed and filled twice with 35 μL 0.1 % Triton X-100 in PBS for no more than 3 min. Then, for each sample a proximity ligation assay was performed following the Duolink® PLA Fluorescence Protocol with Duolink™ In Situ PLA® Probe Anti-Rabbit PLUS (Sigma-Aldrich, Cat. DUO92002), Duolink™ In Situ PLA® Probe Anti-Mouse MINUS (Sigma-Aldrich, Cat. DUO92004), Duolink™ In Situ Detection Reagents FarRed (Sigma-Aldrich, Cat. DUO92013), Duolink™ In Situ Wash Buffers, Fluorescence (Sigma-Aldrich, Cat. DUO82049) and Duolink™ In Situ Mounting Medium with DAPI (Sigma-Aldrich, Cat. DUO82040). The primary antibodies of PRDX1 and ASK1 used in this experiment after blocking were diluted at a 1:350 ratio and incubated overnight at 4 °C. Cell fluorescence images were captured using the Eclipse Ti2 Inverted Microscope (Nikon) with a Far-Red filter set.

PLA images were analyzed using ImageJ. For each PLA image, the number of nuclei stained by DAPI was counted and the total PLA signal area (TotalPLA) was measured at threshold Min.=1000 to Max. The PLA signal from samples without primary antibodies was measured as the background signal (Totalbackground). Then $\frac{PLA\ foci}{nucleus} = \frac{Total\text{PLA} - Total\text{background}}{number\ of\ nuclei}$ was calculated for each PLA image.

Co-immunoprecipitation

Prior to co-immunoprecipitation, lysates were pre-cleared using Protein G Dynabeads™ (Invitrogen, Cat. 10003D) washed five times with PBS. 50 μl of 50 % bead slurry were added to 620 μg of cell lysate (prepared as described above) and incubated on a rotating mixer for 40 min at 4 °C. The supernatant was then collected and requantified by Bradford.

To conjugate the Dynabeads to the anti-PRDX1 antibody, 50 μl of 50 % Dynabead slurry per reaction were washed in PBS as described above, resuspended in PBS-0.02 % Tween with 2.5 μg antibody (Ab) and incubated for 1 h at RT with rotation. The supernatant was subsequently removed and the Dynabeads-Ab complex was washed three times with PBS-0.02 % Tween. The complex was then washed twice with conjugation buffer (20 mM $NaPi_i$, 0.15 M NaCl, pH 7.4) and incubated with 5 mM BS^3 (bis(sulfosuccinimidyl)suberate) (ThermoFisher Scientific, Cat. 21,580) for 30 min at RT with rotation. The cross-linking reaction was

quenched by adding Tris–HCl, pH 7.5 to a final concentration of 50 mM and incubating for a further 15 min at RT with rotation. Finally, the cross-linked Dynabead-Ab complex was washed three times with PBS with 0.1 % Tween.

The cross-linked Dynabead-Ab complex was then added to 600 μg pre-cleared cell lysate and incubated for 4 h at 4 °C with rotating. The Dynabeads were then washed three times with PBS with 0.1 % Tween. After the final wash, the beads were again resuspended in PBS with 0.1 % Tween and transferred to a fresh tube. Elution was performed by resuspending the beads in 20 μl of 50 mM glycine, pH 2.5, vortexing briefly and incubating for 5 min at RT with gentle shaking. The supernatant was removed and the procedure repeated. The combined supernatants were neutralised by adding Tris, pH 10 to a final concentration of 50 mM.

The co-immunoprecipitation was performed with $n = 1$.

Mass spectrometry

The immunoprecipitation eluates were alkylated by 25 mM chloroacetamide and proteins precipitated by methanol/chloroform extraction. The pellet was dissolved in 50 mM NH_4HCO_3 pH 8.0 and digested overnight at 37 °C with 1 μg trypsin (Promega). The reaction was stopped by adding TFA (0.1 % v/v). Peptides were separated by nano-LC as described [30] using a C18 Pepmap precolumn (ThermoScientific) and a Biozen C18 analytical column 0.075 × 25 cm (Phenomenex). Mass spectrometry was performed on an Orbitrap Tribrid Fusion Lumos (ThermoScientific) with a data dependent scan routine with charge state specific fragmentation. For ions with charges above +4 EThcD, HCD for +2 and +3 full scan resolution was set at 120.000 and all MS2 scans were acquired at 30.000. The resulting MS/MS data was processed using Sequest HT search engine within Proteome Discoverer 2.5 SP1 against a *Mus musculus* protein database obtained from Uniprot. Trypsin was specified as a cleavage enzyme allowing up to 2 missed cleavages, 4 modifications per peptide and up to 8 charges. Mass error was set to 10 ppm for precursor ions and daughter ions. Oxidation on Met (+15.995 Da), conversion of Gln (−17.027 Da) or Glu (- 18.011 Da) to pyro-Glu-at the peptide N-term were considered as variable modifications. False discovery rate (FDR) was assessed using Percolator and thresholds for protein, peptide and modification site were specified at 1 %. For abundance comparison, abundance ratios were calculated by Label Free Quantification (LFQ) of the precursor intensities within Proteome Discoverer 2.5 SP1, normalisation was done on PRDX1 level. Potential mixed disulphides were searched with pLink2 against the same mouse database [31].

Data analysis

Graphpad Prism (GraphPadSoftware, version 9.3.1) was used for statistical analysis and graphical representation of the data. The statistical methods used were one-way and two-way ANOVA, and Tukey's multiple comparison test (the precise test is indicated in the figure legend). The data are displayed as either mean ± SE, mean ± SD, or the individual points. A minimum significant level of $p = 0.05$ was set. In the case of the Prdx2 dimerisation data, we employed a logistic regression model of the form Constant + Replicate + Macrophage + Treatment + Macrophage.Treatment was fitted to the % Prdx2 dimer data, using Genstat v22 (VSN international). The dispersion parameter for the variance of the response was estimated from the residual mean square of the fitted model. Wald statistics were used to assess the significance of the main effects macrophage and treatment and its interaction term, by dropping these fixed terms from the full model. T-statistics were used to assess the significance of treatment effects (on the logit transformed scale) by pairwise comparisons.

The mass spectrometry hits were first analyzed using Venny v2.1 (https://bioinfogp.cnb.csic.es/tools/venny/) to find unique and common interactors of the three macrophage polarisation states. STRING v11.5 (http://string-db.org) was then used to map PRDX1-identified proteins interaction networks and enrich for biological pathways.

Results and discussion

The gene expression level of several key antioxidant enzymes is elevated in M1 macrophages, with PRDX1 and PRDX5 being most prominent

To evaluate the differences in expression level of Prdxs and other antioxidant enzymes in differentially polarised macrophages, we exposed isolated BMDMs to LPS/IFN−γ to polarise them towards the M1 phenotype, and IL-4 to polarise them towards the M2 phenotype. Successful polarisation was verified by assessing the expression levels of polarisation-related genes via qRT-PCR: nitric oxide synthase 2 (*Nos2*) for M1 and arginase-1 (*Arg1*) for M2 (Fig. 1**A**). We next compared mRNA levels of all 6 Prdxs by qRT-PCR and found that, apart from *Prdx4*, all Prdxs were upregulated in M1 macrophages, with *Prdx1* and *Prdx5* displaying the most significant increase in expression (Fig. 1**B**). One potential reason why *Prdx4* is not upregulated in M1 macrophages could be its non-immune role, as it is strictly localized within the lumen of the endoplasmic reticulum (ER), where it scavenges H_2O_2 generated during oxidative protein folding [32].

The particularly strong, relative to other Prdxs, upregulation of *Prdx1* and *Prdx5* in M1, despite all Prdxs having similar second-order rate constants, could potentially be related to their proven functions in macrophages, which are not only mediated by their H_2O_2 scavenging capacity, but also by their signaling role. For example, in macrophage-derived foam cells, PRDX1 was found to decrease ROS levels, while also regulating p38 activation, potentially protecting cells from necrosis upon the onset of oxidative stress [27]. Likewise, PRDX5 has been reported to negatively regulate IL-6, which stimulates polarisation to M2, via direct inhibition of the Jak2-Stat5 pathway [33,34]. In this study we decided to not further assess PRDX5, as its role in polarized macrophages has already been thoroughly investigated [28], unlike that of PRDX1.

In line with the mRNA data, PRDX1 protein levels were significantly increased in M1 as compared to M0, while M2 did not upregulate this enzyme (Fig. 1**C**). PRDX2, which is also a typical cytosolic 2-Cys-Prdx with 89 % sequence similarity and 74 % sequence identity to PRDX1 in mice [35], was also significantly upregulated in M1 cells (albeit to a lesser extent than PRDX1, also in accordance with the mRNA data), but not in M2 cells.

Finally, as Prdxs are recognised as transcriptional targets of the murine Nrf2 orthologue NFE2L2 [36,37], we also assessed the expression levels of other NFE2L2 targets involved in the antioxidant response. These included glutathione synthetase (*Gss*), heme oxygenase-1 (*Hmox1*), as well as *Nfe2l2* itself, and its negative regulator *Keap1* [36] (Fig. 1**D**). In addition, we measured the expression of catalase (*Cat*), and thioredoxin 1 (*Txn1*). The latter recycles Prdxs, allowing them to participate in a new H_2O_2-scavenging cycle, and could therefore indirectly impact the levels of H_2O_2 within the cell. We found that *Gss, Hmox1, Keap1* and *Txn1* are all upregulated in M1 cells, while catalase expression is unaltered in all macrophage activation states. While both catalase and Prdxs are known to react with H_2O_2 with second-order reaction rate constants in the 10^7–10^8 $M^{-1}s^{-1}$ range [38], they differ in their K_M for H_2O_2 by a 1000-fold, with catalase having a K_M in the mM range, and PRDX1 having a K_M in the μM range [39,40]. Moreover, unlike most Prdxs, catalase is restricted to peroxisomes [38]. Thus, while all macrophage activation states express catalase for scavenging high H_2O_2 concentrations in peroxisomes, only M1 macrophages harbour efficient cytosolic antioxidant enzymes in the form of PRDXs.

Steady-state H_2O_2 levels are lower in M1 than in M0 and M2 macrophages

Although we do not directly demonstrate the translocation of NFE2L2 to the nucleus or KEAP1 inactivation, the elevated expression of

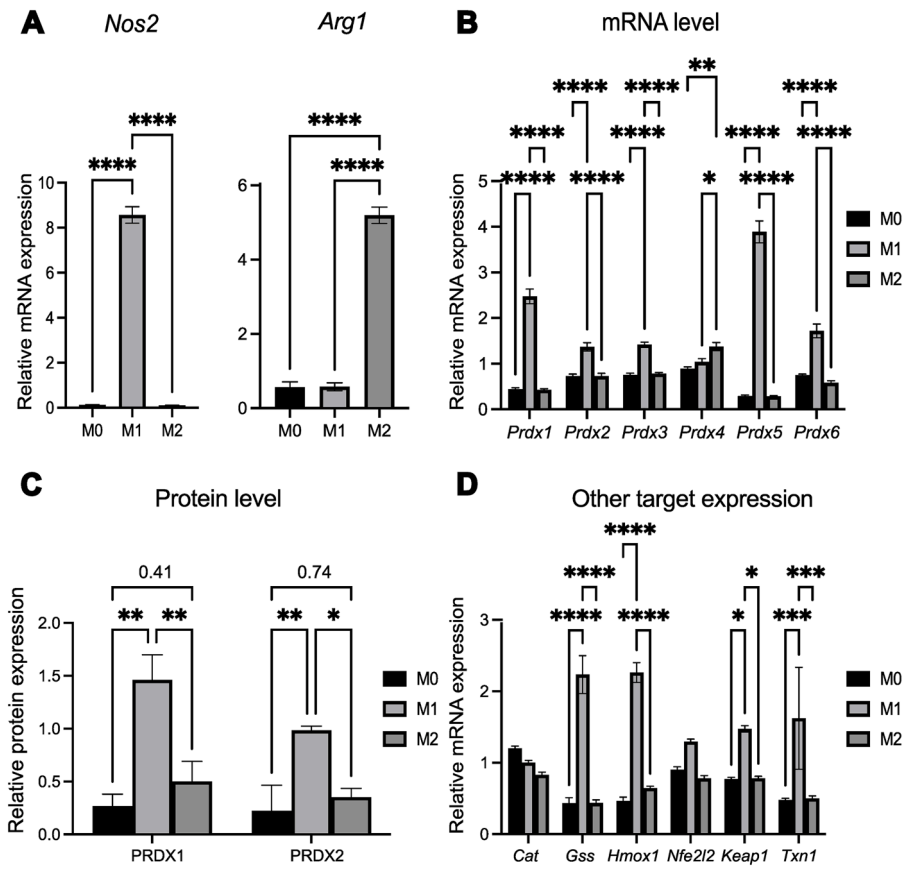

Fig. 1. Bone marrow-derived macrophages were successfully polarized to the M1 and M2 phenotype. M1 macrophages display higher expression levels of several key antioxidant enzymes. (A) The expression levels of the M1 marker *Nos2* and of the M2 marker *Arg1* were assessed by qRT-PCR. (B) mRNA expression level of Prdxs relative to the reference gene S12, as determined by qRT-PCR. (C) PRDX1 and PRDX2 protein expression levels normalised to GAPDH, as quantified from a western blot against PRDX1 and PRDX2, a representation of which is presented in Fig. 3D, with the remaining uncropped blots in Fig. S2. (D) The mRNA expression level of several other tested NFE2L2 (murine Nrf2 orthologue) targets relative to the reference gene S12, as determined by qRT-PCR. *Cat* – catalase; *Gss* – glutathione synthase; *Hmox1* – heme oxygenase-1; *Txn1* – thioredoxin1. The results in all panels are representative of $n = 3$ independent experiments. The bars represent the mean ± SE for (A), (B) and (D), and the mean ± SD for (C). * $p \leq 0.1$; ** $p \leq 0.01$; *** $p \leq 0.001$; **** $p \leq 0.0001$. The p-value is based on Tukey's multiple comparisons test of a one-way ANOVA.

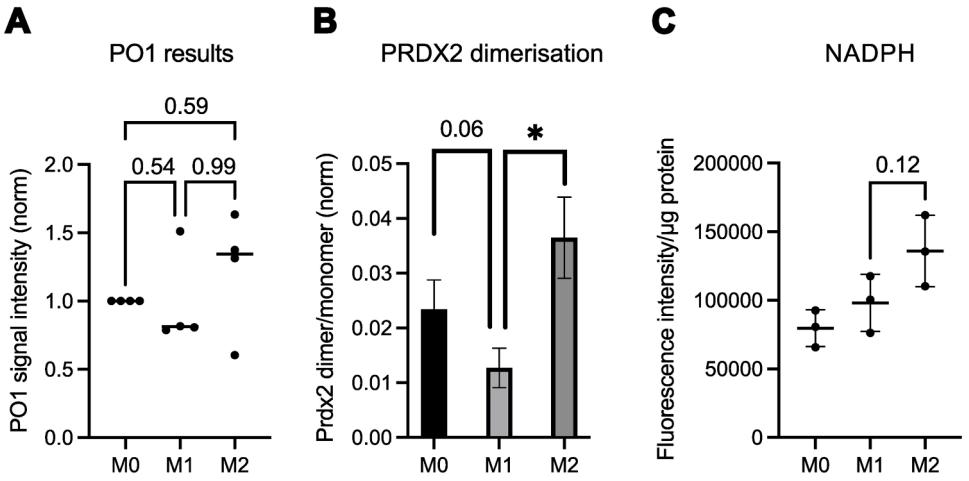

Fig. 2. Cytosolic H_2O_2 levels are lower in M1 than in M0 and M2 macrophages, while NADPH levels do not differ. (A) H_2O_2 quantification using Peroxy Orange 1. The intensity was measured by FACS and normalised to the value of M0. (B) Quantification of the PRDX2 dimer/monomer ratio in a non-reducing western blot. The bars represent the mean and the error bars the SEM. The values were derived from the blot portrayed in Fig. 3**B**, and the uncropped in **Fig. S2**. (C) NADPH concentration in different macrophage subtypes. The results in all panels are representative of at least $n = 3$ independent experiments. For A and C, all points are presented individually, and the horizontal bar represents the median. Ns – not significant, .* $p \leq 0.05$. The p value is based on Tukey's multiple comparisons test of a one-way ANOVA (A and C) and Wald statistics (B).

multiple NFE2L2 target genes in M1 macrophages implies that NFE2L2 is not being degraded and is active. This would only be possible upon KEAP1 inhibition, which H_2O_2, a known physiological KEAP1 inhibitor, can achieve [41]. Hence, we hypothesised that M1 macrophages have increased H_2O_2 levels. We directly tested this hypothesis using a boronate-cage H_2O_2-specific dye, Peroxy Orange 1 [42], but observed no significant differences between M0, M1 and M2 cells **(**Fig. 2**A).**

The fact that Peroxy Orange 1 responded to exogenous treatment with 100 μM H_2O_2 though (**Fig. S1**), suggested that this dye could simply not be sensitive enough to detect differences between the subtypes. To our knowledge, the limit of detection of Peroxy Orange 1 has not been determined, but likely lies in the 100–200 nM range, as, taking into account that the gradient between extracellular and intracellular H_2O_2 is about 390-fold [43], 100 μM of exogenous H_2O_2 would correspond to approximately 250 nM in cells. As endogenous steady-state H_2O_2 levels are lower, namely below 10 nM [44], it is very likely that differences in H_2O_2 levels between the macrophage subtypes, if they exist, would be in that range. To this end, we next used a more sensitive technique – the assessment of the degree of PRDX2 dimerisation using a non-reducing western blot, where increased dimerisation is indicative of elevated H_2O_2 levels [45]. This feature of Prdx2 has served as the basis for a fluorescent H_2O_2 biosensor [46], which was shown to respond to 1 μM of exogenously added H_2O_2., which, considering a 390-fold gradient, equates to 2.5 nM intracellularly. In this case, we observed a significant decrease in PRDX2 dimerisation in M1 cells compared to M0 and M2 (the p-value for M0 vs M1 is almost significant, being 0.0582) **(**Fig. 2**B).** In fact, the Peroxy Orange 1 data, though statistically insignificant, is also in line with these results, with the signal intensity being lower in M1 cells **(**Fig. 2**A).** These results suggest that the increased expression of antioxidant enzymes, including PRDXs, TXN1, and GSS, in M1 macrophages very efficiently scavenges excess H_2O_2, resulting in H_2O_2 levels even lower than those in M0 and M2 macrophages. While this finding might seem counterintuitive, especially considering the role of M1 macrophages in anti-microbial and anti-tumour activities via ROS [2], it becomes less surprising if we consider the mechanism of H_2O_2 production in macrophages. Indeed, H_2O_2 in macrophages is not produced constantly, but only following stimulation in a process known as "oxidative burst", wherein superoxide ($O_2^{\cdot-}$) is generated by the phagosomal NADPH oxidase NOX2. This $O_2^{\cdot-}$, in turn, is then rapidly converted to H_2O_2 [47,48]. Additionaly, both H_2O_2 detection methods we employed mainly detect cytosolic H_2O_2, while there is growing evidence indicating that mitochondrial H_2O_2 also significantly contributes to the phagocytic response of macrophages [49].

Finally, as intracellular H_2O_2 levels are also regulated by the reducing systems of the cell, i.e. the thioredoxin and glutathione/glutaredoxin systems which both use NADPH as electron source, we compared the NADPH levels in the different macrophage activation states **(**Fig. 2**C).** However, no significant differences were found, despite the high flux of the pentose phosphate pathway that characterizes M1 macrophages [50].

Increasing the H_2O_2 levels increases PRDX1 but not PRDX2 expression levels

Our data suggest that M1 macrophages have higher expression levels of antioxidant enzymes to protect against rapid elevations of H_2O_2 levels in these cells. Therefore, we hypothesised that experimentally altering H_2O_2 levels would impact the expression of *Prdx*.

To test this assumption, we treated cells with auranofin, a thioredoxin reductase (TrxR) inhibitor that hinders the recycling of Prdx and consequently results in an increase in H_2O_2 levels [51]. In addition, we employed Trolox, a frequently used antioxidant. While Trolox is unlikely to directly scavenge H_2O_2, it could do so indirectly, by decreasing the burden on the antioxidant systems of the cell. For example, GPX4, which scavenges lipid peroxides, depends on the glutathione system and ultimately NADPH for its recycling; hence a decrease in NADPH consumption to recycle GPX4 would make more reducing equivalents available for recycling PRDXs, thus lowering H_2O_2. As a readout for changes in H_2O_2 levels, we again measured PRDX2 dimerisation (Fig. 3**A**). We selected Trolox over another widely-used antioxidant, N-acetyl cysteine (NAC), because NAC acts as a source of per- and polysulfides [52], triggering Prdx2 dimerisation [53], and as a consequence making NAC incompatible with our measurement technique. While we detected a significant increase in PRDX2 dimerisation in M0, M1 and M2 upon auranofin treatment as compared to the untreated conditions, Trolox treatment did not affect PRDX2 dimerisation. This may indicate that lipid peroxidation is not burdening the cell, or simply that Trolox cannot lower steady state H_2O_2 levels further.

As we did not observe an effect of Trolox treatment, we decided to only use auranofin treatment in subsequent experiments. As an important control, we first checked whether auranofin affects macrophage polarisation, using the same M1/M2 marker genes as before. As can be seen in Fig. 3**B**, auranofin treatment did not affect the LPF/IFNγ− or IL-4-induced polarisation state. We then assessed whether auranofin treatment would affect *Prdx1* and *Prdx2* expression. While *Prdx2* expression continued to remain low in all three polarization states and, if anything, even decreased upon auranofin treatment, auranofin increased *Prdx1* expression levels in M0 and M2 cells to bring them on par with those of M1 **(**Fig. 3**C).** We also analyzed whether these changes in gene expression would be reflected at the protein level **(**Fig. 3**D).** PRDX1 expression increased in M0 cells (albeit not significantly ($p = 0.097$), in line with the mRNA data. In contrast, in M1 cells, and to a lesser extent, in M2 cells, PRDX1 protein levels decreased, contrary to what was observed at the mRNA level. As for PRDX2, we did not observe any differences between treated and untreated cells in any of the macrophage subtypes. It is not uncommon to find a lack of consistency between mRNA and protein expression levels [54]. This can be attributed to factors such as post-transcriptional and translational regulation, as well as differences in mRNA and protein turnover rates [55]. Moreover, in the particular case of PRDXs, which serve not only as H_2O_2 scavengers but also play a role in signalling, this might indicate a post-translational process to prevent unintended signalling activation when PRDX is produced as part of a broad antioxidant transcriptional responses.

We next assessed how auranofin affects the expression of two more antioxidant genes whose expression we analyzed in Fig. 1**D**: one gene (*Cat*) where expression levels did not differ among the cells, and another (*Txn1*) where there was a difference **(**Fig. 3**E).** In the case of *Cat,* the expression levels increased in macrophages of all polarisation states, while for *Txn1*, they increased in the case of M0 cells and decreased in M1 cells. These results suggest that catalase starts playing a more important role in H_2O_2 elimination across all macrophage subtypes upon the inhibition of PRDX recycling. Most likely, catalase is just one of the H_2O_2 scavenging enzymes whose expression level increases upon auranofin treatment. We would particularly expect the levels of those enzymes that do not depend on the thioredoxin system for recycling, such as the glutathione peroxidases, to increase.

The interaction between PRDX1 and ASK1 is most prominent in M1 cells

As previously mentioned, PRDX1 plays a dual role in macrophage-derived foam cells, serving not only as an H_2O_2 scavenger but also as a signalling protein [27]. The best-characterised interaction partner of PRDX1 is the kinase ASK1 [21,22], which is also responsible for the PRDX1-dependent phosphorylation of p38 observed by Conway et *al.* in foam cells. We therefore evaluated whether high *Prdx1* levels in untreated M1 macrophages, or their increase in all polarization states post-auranofin treatment, would translate to an increase of the PRDX1-ASK1 interaction.

First, ASK1 expression levels at both the mRNA and protein levels were assessed in M0, M1 and M2 macrophages **(**Fig. 4**A).** *Map3k5* mRNA expression (encoding for ASK1) was highest in unpolarised macrophages

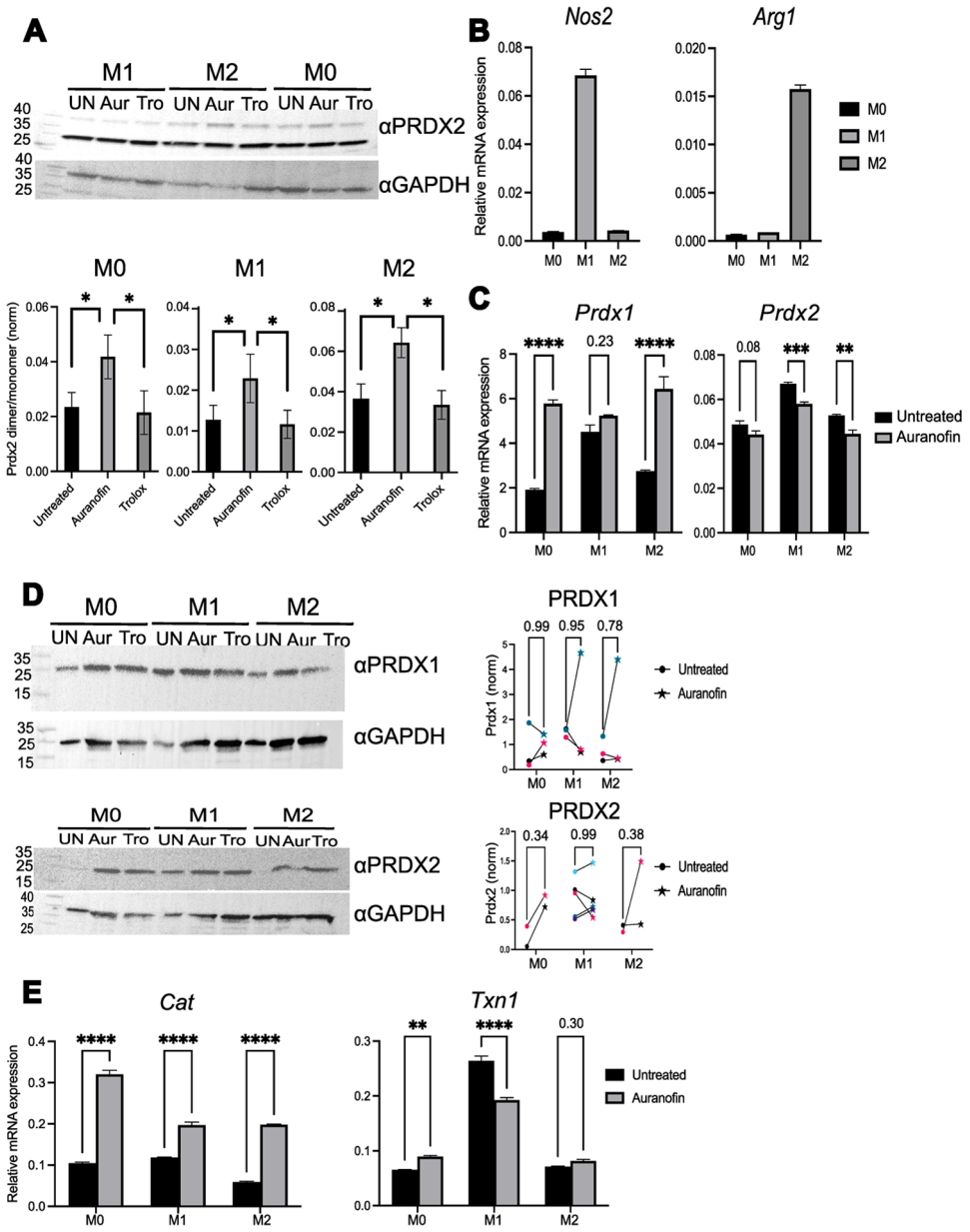

Fig. 3. Elevation of H_2O_2 levels does not affect cell polarisation, but increases *Prdx1* but not *Prdx2* expression levels (A) Representative picture of a non-reducing anti-PRDX2 western blot with GAPDH as a loading control with a quantification of the PRDX2 dimer/monomer ratio normalized to GAPDH. The bars represent the mean and the error bars the SEM. The other two replicates, as well as an uncropped version of the blot are presented in **Fig. S2**. The numbers on the left of the blot represent size markers in kDa. (B) The expression levels of the M1 marker *Nos2* and of the M2 marker *Arg1* after auranofin treatment, as assessed by qRT-PCR, normalized to S12 expression. (C) Expression level of *Prdx1* and *Prdx2* relative to the reference gene S12, as determined by qRT-PCR. (D) Representative picture of an anti-PRDX1 and anti-PRDX2 reducing western blot with GAPDH as a loading control. The other replicate, as well as an uncropped version of the blot, is presented in **Fig. S3.** The numbers on the left of the blot represent size markers in kDa. The graphs are a quantification of the western blot normalised to GAPDH. The bars represent the mean and the error bars the SEM. (E) Expression level of Cat and Txn1 relative to the reference gene S12, as determined by qRT-PCR. The bars represent the mean ± SE. The results in all panels except for (D) are representative of $n = 3$ independent experiments (for D $n = 4$ for PRDX1 and $n = 2$ or more for PRDX2). The p-value is based on Tukey's multiple comparisons test of a two-way ANOVA in all except A and D, where Wald statistics were used. Ns – not significant; * $p \leq 0.1$; ** $p \leq 0.01$; *** $p \leq 0.001$; **** $p \leq 0.0001$.

and lowest in M1 macrophages. This pattern is maintained at the protein level. We then determined the PRDX1:ASK1 interaction by a Proximity Ligation Assay (PLA) (Fig. 4**B**), showing that this interaction is clearly more prominent in M1 and M0 cells as compared to M2. The fact that we observed as many PRDX1:ASK1 interaction foci in M0 cells as in M1 cells, despite M1 cells having much higher PRDX1 expression levels suggests that the reason for detecting more PRDX1:ASK1 interaction foci in M1 cells is not solely due to increased PRDX1 expression. It is worth noting that PLA results can only indicate whether the proteins are in close enough proximity (<40 nm) for the reaction to occur [56], but does not prove whether PRDX1 and ASK1 are productively engaged in a redox relay. To obtain a first indication of this, we analyzed the expression of genes whose expression is ultimately the result of ASK1 activation. We selected three targets of cJUN, a transcription factor that is activated downstream of ASK1, via JNK [57]: cyclooxygenase 2 (*Cox2*) [58,59], indoleamine-2,3-dioxygenase 1 (*Ido1*) [59] and tumor necrosis factor (*Tnf*) [60]. As can be seen in Fig. 4**C,** *Cox2* and *Tnf* were expressed in M1 macrophages at much higher levels than in the other

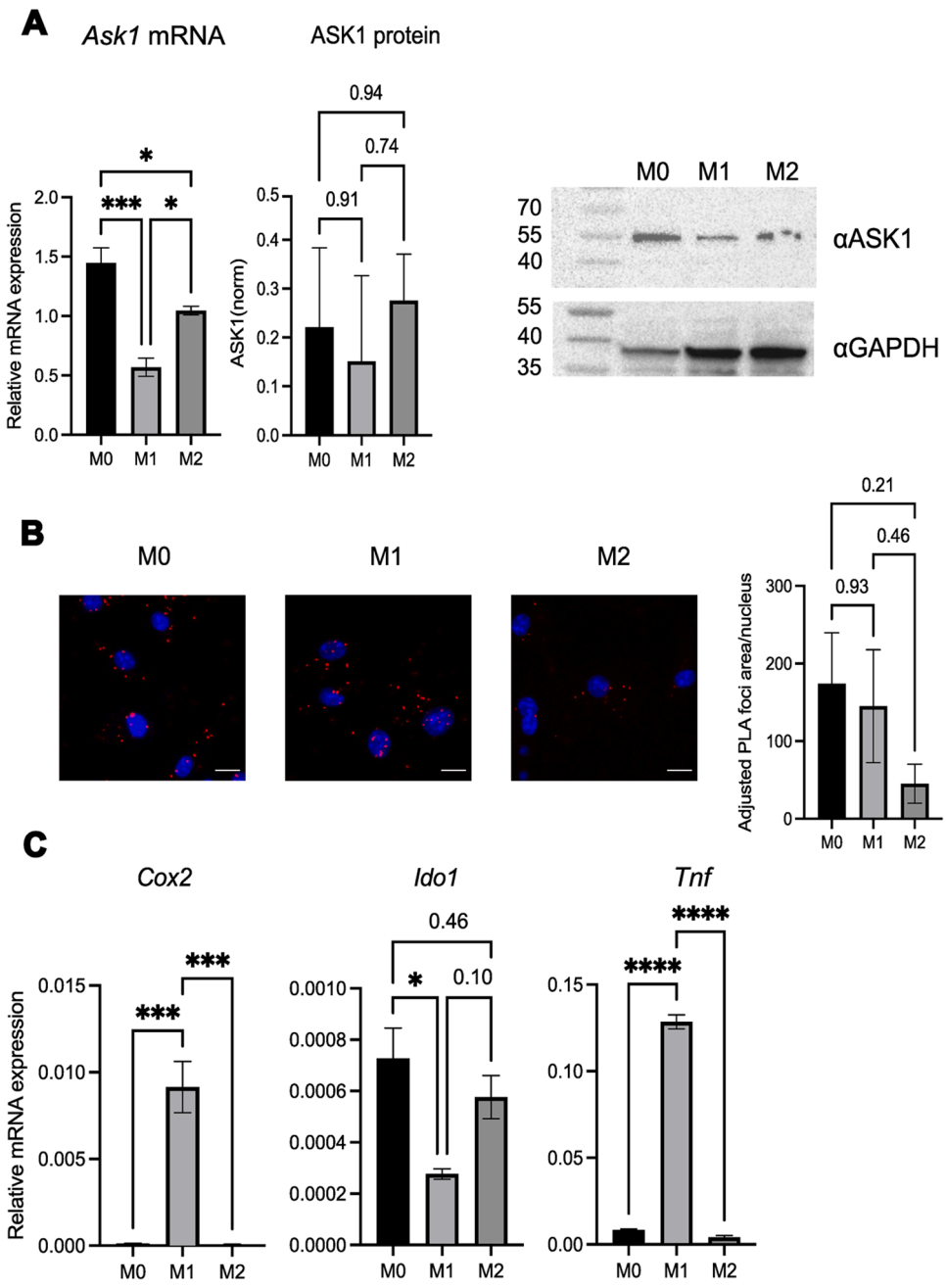

Fig. 4. The PRDX1:ASK1 interaction is most prominent in M1 cells. (A) mRNA expression level of *Map3k5 (Ask1)* relative to the reference gene S12, as determined by qRT-PCR, and protein expression levels normalised to GAPDH as determined by western blot. The other two replicates, as well as the uncropped blot are presented in **Fig. S4**. (B) Representative pictures of the PLA assay results using anti-PRDX1 and anti-ASK1 primary antibodies, and their quantification. The red foci represent each interaction, and the nuclei are stained in blue. (C) Expression levels of selected genes downstream of ASK1: *Cox2, Ido1* and *Tnf*. The results in all panels are representative of $n = 3$ independent experiments. The bars represent the mean ± SE for the qPCR results and the mean ± SD for other experiments. The p-value is based on Tukey's multiple comparisons test of a one-way ANOVA. * $p \leq 0.1$; ** $p \leq 0.01$; *** $p \leq 0.001$; **** $p \leq 0.0001$; ns - non-significant.

activation states. On the other hand, for *Ido1* we observed the opposite. This could potentially be explained by the fact that in mice, NF-κB also regulates *Ido1* expression [61], and ASK1 suppresses NF-κB [62]. Disentangling NF-κB vs cJUN-mediated transcriptional regulation of *Ido1* is, however, beyond the scope of this study. It should be stressed that these results are only indicative of ASK1 being active, as an increase in the expression of these genes can also be elicited by other factors, Thus, it seems that while PRDX1 and ASK1 are located closer than 40 nm from each other in both M0 and M1 macrophages, they are forming a redox relay only in M1 macrophages, potentially because the H_2O_2 needed to launch the relay is only produced in M1 macrophages. However, we can also not rule out that ASK1 could simply have different targets in M0 macrophages which we do not test here.

The PRDX1:ASK1 interaction tends to increase in M2 macrophages upon an elevation of H_2O_2 levels

After showing that auranofin treatment tended to lead to an altered PRDX1 protein expression in all macrophage polarization states, we investigated whether this would translate to a change in the PRDX1:ASK1 interaction frequency (Fig. 5**A**). We found no difference in PRDX1:ASK1 interactions in M0 and M1 cells, but a trend towards an increase in

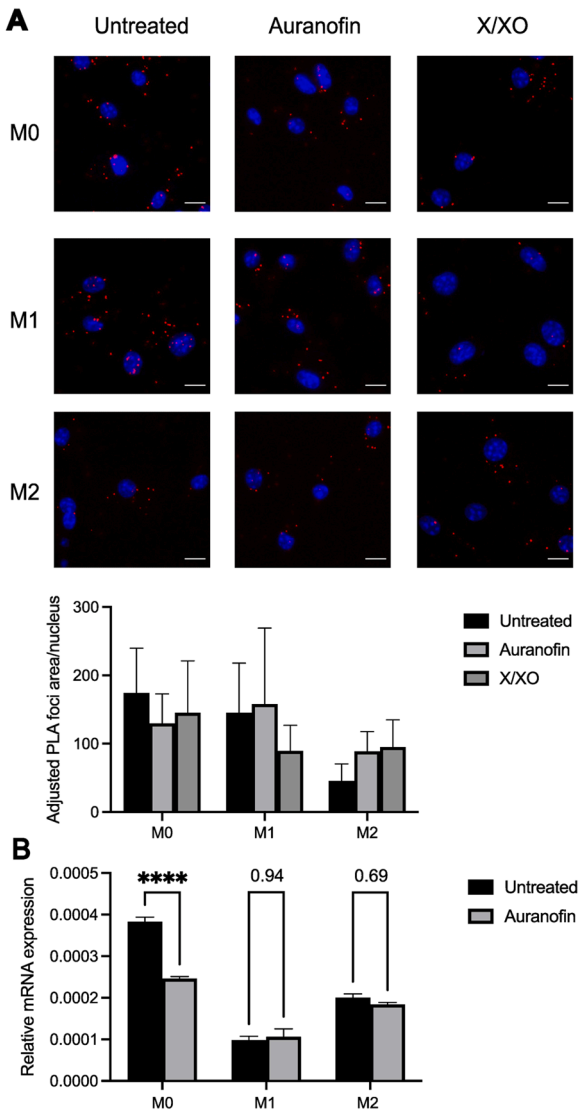

Fig. 5. The PRDX1:ASK1 interaction depends on H_2O_2 levels. (A) Representative pictures of the PLA assay results using anti-PRDX1 and anti-ASK1 primary antibodies, and their quantification. The red foci represent each interaction and the nuclei are stained in blue. The untreated samples are replicated from Fig. 4B. Results are not statistically significant. (B) Expression levels of *Ask1*1 relative to the S12 gene before and after Auranofin treatments, as assessed by qRT-PCR. The results in all panels are representative of $n = 3$ independent experiments. The bars represent the mean ± SE for the qPCR results and the mean ± SD for PLA experiments. The p-value is based on Tukey's multiple comparisons test of a two-way ANOVA. * $p \leq 0.1$; ** $p \leq 0.01$; *** $p \leq 0.001$; **** $p \leq 0.0001$; ns - non-significant.

M2 cells. To strengthen these findings, we also exposed cells to another source of H_2O_2: xanthine/xanthine oxidase (X/XO) [63]. A similar PRDX1:ASK1 interaction pattern was observed. As PRDX1 protein levels tended to decrease post-auranofin treatment in M2 cells **(**Fig. 3**D)**, the increase in PLA foci could not be explained merely by an increase in the levels of one of the interacting partners. To get an indication of changes in the expression of the other partner - ASK1, we assessed its expression at mRNA level **(**Fig. 5**B)**. While we observed no changes in *Ask1* expression level in M1 and M2 macrophages, there was a significant decrease in M0 macrophages. These results suggest that the formation of PLA foci is not related to PRDX1 and ASK1 expression levels.

PRDX1 interacts with targets involved in the oxidative stress response in M1 but not in M2 cells

Taken together, our results suggest that macrophages use PRDX1 to combat elevated H_2O_2 levels by both scavenging H_2O_2, as well as by eliciting a cellular adaptation response as exemplified by its interaction with ASK1. To gain an overall view on other interaction partners of PRDX1, we next performed a PRDX1-pulldown and identified the interactors with mass spectrometry. We found 107 interaction partners for M1 cells and 104 for M2 cells, of which 72 were common to both, including PRDX1 itself **(**Fig. 6**A, Suppl. File 2)**. We then searched for mixed disulphides but we did not obtain any hits involving PRDX1. This outcome is not surprising, as Prdxs have previously been reported to be part of complexes where not all proteins are covalently linked [24,64]. Moreover, our lab has also used a thiol-independent technique to identify interactors that are not predicted to form disulphides with PRDX2 [65].

To categorise the identified proteins based on their biological GO terms, as well as to position them within networks of their known interaction partners, we projected the proteins unique to each polarisation status to the STRING database. For M1 macrophages, we found that some of our identified PRDX1 interaction partners have previously been predicted (edges connecting PRDX1 with other proteins) **(**Fig. 6**B, Suppl. Table 2)**. Among the proteins uniquely found in M1 were Parkinson disease 7 (PARK7), alpha-enolase (ENO1), and cytochrome P450 2E1 (CYP2E1), which have all been implicated in cellular protection from or regulation of oxidative stress [66–68]. The four most enriched GO terms for the identified interactors in M1 macrophages indicate their involvement in ROS metabolic processes (Table 1). The interactors could work together with PRDX1 to maintain the cytosolic H_2O_2 levels no higher (or even lower, according to Fig. 2**B**) than those in other polarisation cell types. In agreement with this hypothesis, a study that used a combination of high-throughput metabolomics and transcriptomics to compare the metabolo-transcriptional network of M1 and M2 cells [69] reported increased levels of glutathione reductase (*Gsr*) and oxidized glutathione (GSSG) in M1 cells compared to M2 cells. This end goal of this may be to prepare for the consequences of a NOX2-mediated oxidative burst upon stimulation.

By contrast, none of the identified PRDX1 interactors in M2 macrophages was associated with ROS, with most interactors described by the "cytoplasmic translation" term **(**Fig. 6**C, Suppl. Table 3)**. Proteins that formed direct edges with PRDX1 included malate dehydrogenase 2 (MDH2), the ATP synthase subunit 5o (ATP5O) and the voltage-dependent anion-selective channel protein 2 (VDAC2) – all mitochondrial proteins, which is consistent with the reliance of M2 macrophages on mitochondrial oxidative phosphorylation, in contrast to M1 macrophages that prefer aerobic glycolysis for ATP production. A notable exception in the M2 PRDX1 interactome was superoxide dismutase 1 (SOD1). Proteins identified in both M1 and M2 cells (**Fig. S5, Suppl. Table 4**) were mainly related to the ribosomal assembly and translation GO terms. Furthermore, STRING-predicted PRDX1 interactors included proteins involved in both mitochondrial respiration – the ATP synthase subunit 5a1 (ATP5A1) and glycolysis – pyruvate kinase (PKM), as well as catalase.

To validate the results of the identified differences observed by mass spectrometry, we compared the expression levels of a protein that was only identified to be a PRDX1 interactor in one of the macrophage subtypes, in whole cell lysates. Our rationale was that if we observe no significant differences in expression of this target between the macrophages, it would suggest that its identification in the IP must be due to its association with PRDX1 and not, for example, due to inadequate washing away of a highly abundant protein in that subtype. We selected PARK7 as such a target, as it was identified as a PRDX1 interaction partner in M1, but not in M0 and M2 macrophages. Our western blot revealed no significant differences in PARK7 expression between the macrophages, hence its identification as a PRDX1 target exclusively in

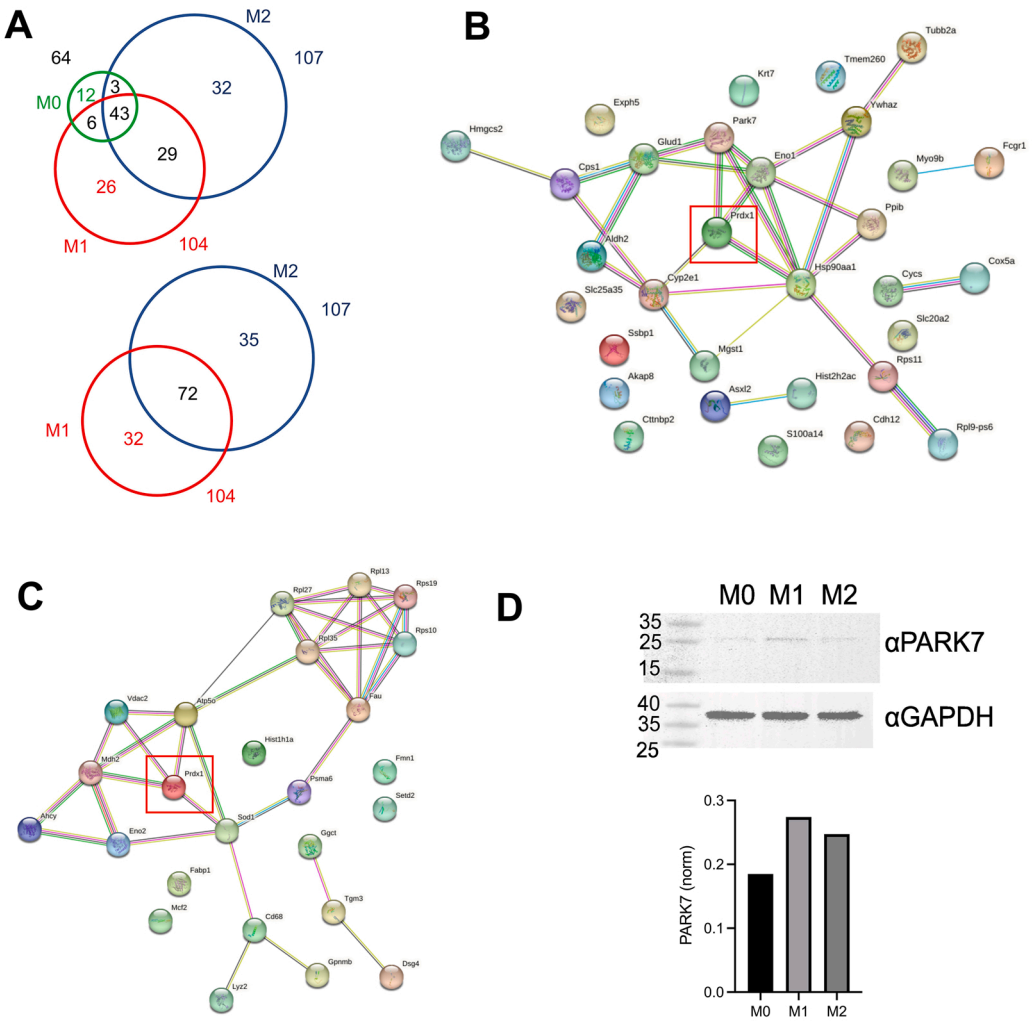

Fig. 6. PRDX1 interacts with targets involved in the oxidative stress response in M1 but not in M2 macrophages. (A) Venn diagrams depicting the number of PRDX1 targets identified by mass spectrometry in all three polarisation states, and for M1 and M2 alone. The numbers outside the circles are the total number of proteins identified. The diameter of the circles is proportional to the number of hits. (B) PRDX1 interaction network with the unique identified hits generated by STRING in M1 macrophages. PRDX1 is marked by a red box. (C) PRDX1 interaction network with the unique identified hits generated by STRING in M2 macrophages. PRDX1 is marked by a red box. (D) Expression of PARK7 as assessed by western blot, and its quantification as normalized to GAPDH. The uncropped blot is presented in **Fig. S6.**

Table 1
Biological process GO terms of PRDX1 interactors identified in M1, M2 or both activation states. The false discovery rate (FDR) is provided in brackets.

M1 macrophages	M2 macrophages	M1 and M2 macrophages
Hydrogen peroxide metabolic process (p=0.0432)	Cytoplasmic translation (0.00298)	Ribosomal small subunit assembly (p=0.0041)
Reactive oxygen species metabolic process (p=0.0046)		Ribosome assembly (p=0.0021)
Cellular detoxification (p=0.0432)		Ribosomal small subunit biogenesis (p=0.0029)
Oxidation-reduction process (p=0.0218)		Translation ($p=6.12 \times 10^{-5}$)

M1 macrophages cannot merely be explained by its abundance (Fig. 6**D**).

Conclusion and perspectives

Although PRDX1 is likely just one of several proteins involved in protecting macrophages from oxidative stress, as evidenced by the upregulation of the catalase expression in all macrophages exposed to auranofin, we nevertheless were able to endow it with a special role. To provide more compelling evidence for the necessity of PRDX1 in macrophage antioxidant defence and redox signalling, we would have had to perform experiments in BMDMs generated from *Prdx1* knock-out mice. Such experiments have already been performed by Jeong and colleagues, who demonstrated that basal intracellular H_2O_2 levels was increased in murine macrophages lacking *Prdx1* [25], despite the presence of other antioxidant enzymes. In our study we built on these findings to show that *Prdx1* overexpression is specific to M1 macrophages, while M2 macrophages upregulate *Prdx1*, but not its close homologue *Prdx2*, when exposed to increased H_2O_2 levels at the mRNA,

but not on the protein level. In addition, we demonstrated that PRDX1 interacts, or at least comes into proximity with, ASK1 in M1 cells at basal levels, and in M2 cells once H_2O_2 levels increase.

These results raise the question of whether inducing *Prdx1* expression could be a target for repolarising M2 cells into M1 cells, offering an exciting new anti-tumor therapeutic opportunity [70]. Strategies to polarise M2 cells to M1 cells, would allow the conversion of M2-like pro-tumour TAMs cell to anti-tumour M1-like cells. Jaynes et al. have already demonstrated the potential of this approach by targeting the mannose receptor CD206, highly expressed in M2-like TAMs, with a synthetic peptide analogue, leading to TAM conversion to a more M1-like phenotype and tumour growth suppression [71]. Further, there are indications that the PRDX1-ASK1 axis could be implicated in TAM repolarisation, as ASK1 knockdown or inhibition in M1 macrophages led to the restoration of the M2 phenotype [72]. Hence, activating ASK1 could do the opposite. The best approach to achieving this remains an open question. Even though our results have shown that, at least in M2 macrophages, an increase in H_2O_2 levels increases the PRDX1:ASK1 interaction/proximity, simply increasing H_2O_2 levels pharmacologically is not a solution, as this might affect the viability of M1 macrophages, as in these cells the antioxidant systems are already charged with coping with H_2O_2, and a further increase could exceed their available supply of electrons. Indeed, M1 BMDMs were found to be more sensitive to radiotherapy than M2 macrophages [73]. In addition, our results **(**Fig. 5**A)** suggest that an elevation of H_2O_2 levels in M1 macrophages does not stimulate the PRDX1-ASK1 interaction. An alternative approach could be to exploit post-translational modifications, such as phosphorylation, which can affect Prdx activity. For instance, phosphorylation of the Ser32 residue of human Prdx1 has been shown to affect its secondary structure and induce its peroxidase function [74]. Therefore, the development of allosteric regulators of PRDX1 activity is a possibility, although further studies involving macrophage polarisation from *Prdx1* knockout mice are needed to test our hypothesis.

CRediT authorship contribution statement

Daria Ezeriņa: Conceptualization, Methodology, Validation, Formal analysis, Investigation, Writing – original draft, Visualization, Supervision. **Trung Nghia Vo:** Formal analysis, Investigation, Visualization. **Ting Luo:** Formal analysis, Investigation, Visualization. **Yvon Elkrim:** Formal analysis, Investigation, Resources. **Anna Escoda Suarez:** Investigation. **Gaëtan Herinckx:** Investigation. **Didier Vertommen:** Formal analysis, Investigation, Resources. **Damya Laoui:** Conceptualization, Writing – review & editing, Supervision, Funding acquisition. **Jo A. Van Ginderachter:** Conceptualization, Writing – review & editing, Supervision, Funding acquisition. **Joris Messens:** Conceptualization, Writing – review & editing, Supervision, Funding acquisition.

Declaration of Competing Interest

The authors declare that they have no known competing financial interests or personal relationships that could have appeared to influence the work reported in this paper.

Data availability

Data will be made available on request.

Acknowledgements

The authors would like to acknowledge Dr. Marnik Vuylsteke for help with the statistical analysis and Tzu-Keng Shen for assistance with western blot development.

Funding

This work was funded with a VIB grant (to J.M.), and the Research Foundation-Flanders–Fonds de la Recherche Scientifique Excellence of Science project no. 30829584 (to J.M and D.V.). T.L. was supported with a Chinese Scholarship Council grant (File No. 201707650018). T.N.V. was supported with a one-year scholarship of the VUB. D.L. and J.V.G are supported by grants from FWO, Kom op Tegen Kanker, Stichting tegen kanker, VIB and Vrije Universiteit Brussel.

Supplementary materials

Supplementary material associated with this article can be found, in the online version, at doi:10.1016/j.arres.2023.100083.

References

[1] D.M. Mosser, J.P. Edwards, Exploring the full spectrum of macrophage activation, Nat. Rev. Immunol. 8 (2008) 958–969.
[2] P.J. Murray, J.E. Allen, S.K. Biswas, E.A. Fisher, D.W. Gilroy, S. Goerdt, et al., Macrophage activation and polarization: nomenclature and experimental guidelines, Immunity 41 (2014) 14–20.
[3] K.C. Kao, S. Vilbois, C.H. Tsai, P.C. Ho, Metabolic communication in the tumor-immune microenvironment, Nat. Cell Biol. 24 (2022) 1574–1583.
[4] Y. Komohara, Y. Fujiwara, K. Ohnishi, M. Takeya, Tumor-associated macrophages: potential therapeutic targets for anti-cancer therapy, Adv. Drug Deliv. Rev. 99 (2016) 180–185.
[5] K. Movahedi, D. Laoui, C. Gysemans, M. Baeten, G. Stange, J. Van den Bossche, et al., Different tumor microenvironments contain functionally distinct subsets of macrophages derived from Ly6C(high) monocytes, Cancer Res. 70 (2010) 5728–5739.
[6] D. Laoui, E. Van Overmeire, G. Di Conza, C. Aldeni, J. Keirsse, Y. Morias, et al., Tumor hypoxia does not drive differentiation of tumor-associated macrophages but rather fine-tunes the M2-like macrophage population, Cancer Res. 74 (2014) 24–30.
[7] Y. Zhang, S. Choksi, K. Chen, Y. Pobezinskaya, I. Linnoila, Z.G. Liu, ROS play a critical role in the differentiation of alternatively activated macrophages and the occurrence of tumor-associated macrophages, Cell Res. 23 (2013) 898–914.
[8] Q. Xu, S. Choksi, J. Qu, J. Jang, M. Choe, B. Banfi, et al., NADPH oxidases are essential for macrophage differentiation, J. Biol. Chem. 291 (2016) 20030–20041.
[9] L.M. Chen, H.Y. Tseng, Y.A. Chen, A.T. Al Haq, P.A. Hwang, H.L. Hsu, Oligo-Fucoidan prevents M2 macrophage differentiation and HCT116 tumor progression, Cancers 12 (2020), https://doi.org/10.3390/cancers12020421.
[10] Q. Wu, A. Allouch, A. Paoletti, C. Leteur, C. Mirjolet, I. Martins, et al., NOX2-dependent ATM kinase activation dictates pro-inflammatory macrophage phenotype and improves effectiveness to radiation therapy, Cell Death Differ. 24 (2017) 1632–1644.
[11] Y. Zhou, K.T. Que, Z. Zhang, Z.J. Yi, P.X. Zhao, Y. You, et al., Iron overloaded polarizes macrophage to proinflammation phenotype through ROS/acetyl-p53 pathway, Cancer Med. 7 (2018) 4012–4022.
[12] S.J. Salpeter, Y. Pozniak, E. Merquiol, Y. Ben-Nun, T. Geiger, G. Blum, A novel cysteine cathepsin inhibitor yields macrophage cell death and mammary tumor regression, Oncogene 34 (2015) 6066–6078.
[13] N. Gul, S. Grewal, M. Bogels, G.J. van der Bij, M.M. Koppes, S.J. Oosterling, et al., Macrophages mediate colon carcinoma cell adhesion in the rat liver after exposure to lipopolysaccharide, Oncoimmunology 1 (2012) 1517–1526.
[14] C.C. Winterbourn, Reconciling the chemistry and biology of reactive oxygen species, Nat. Chem. Biol. 4 (2008) 278–286.
[15] A. Hall, P.A. Karplus, L.B. Poole, Typical 2-Cys peroxiredoxins–structures, mechanisms and functions, FEBS J. 276 (2009) 2469–2477.
[16] G. Ferrer-Sueta, B. Manta, H. Botti, R. Radi, M. Trujillo, A. Denicola, Factors affecting protein thiol reactivity and specificity in peroxide reduction, Chem. Res. Toxicol. 24 (2011) 434–450.
[17] S.G. Rhee, I.S. Kil, Multiple functions and regulation of mammalian peroxiredoxins, Annu. Rev. Biochem. 86 (2017) 749–775.
[18] H.Z. Chae, T.B. Uhm, S.G. Rhee, Dimerization of thiol-specific antioxidant and the essential role of cysteine 47, Proc. Natl. Acad. Sci. U. S. A. 91 (1994) 7022–7026.
[19] H.Z. Chae, S.J. Chung, S.G. Rhee, Thioredoxin-dependent peroxide reductase from yeast, J. Biol. Chem. 269 (1994) 27670–27678.
[20] S. Stocker, M. Maurer, T. Ruppert, T.P. Dick, A role for 2-Cys peroxiredoxins in facilitating cytosolic protein thiol oxidation, Nat. Chem. Biol. 14 (2018) 148–155.
[21] R.M. Jarvis, S.M. Hughes, E.C. Ledgerwood, Peroxiredoxin 1 functions as a signal peroxidase to receive, transduce, and transmit peroxide signals in mammalian cells, Free Radic. Biol. Med. 53 (2012) 1522–1530.
[22] T.N. Vo, J. Malo Pueyo, K. Wahni, D. Ezerina, J. Bolduc, J. Messens, Prdx1 interacts with ASK1 upon exposure to H2O2 and independently of a scaffolding protein, Antioxidants 10 (2021), https://doi.org/10.3390/antiox10071060.
[23] M.C. Sobotta, W. Liou, S. Stocker, D. Talwar, M. Oehler, T. Ruppert, et al., Peroxiredoxin-2 and STAT3 form a redox relay for H2O2 signaling, Nat. Chem. Biol. 11 (2015) 64–70.

[24] D. Talwar, J. Messens, T.P. Dick, A role for annexin A2 in scaffolding the peroxiredoxin 2-STAT3 redox relay complex, Nat. Commun. 11 (2020) 4512.
[25] S.J. Jeong, S. Kim, J.G. Park, I.H. Jung, M.N. Lee, S. Jeon, et al., Prdx1 (peroxiredoxin 1) deficiency reduces cholesterol efflux via impaired macrophage lipophagic flux, Autophagy 14 (2018) 120–133.
[26] T. Ishii, M. Yamada, H. Sato, M. Matsue, S. Taketani, K. Nakayama, et al., Cloning and characterization of a 23-kDa stress-induced mouse peritoneal macrophage protein, J. Biol. Chem. 268 (1993) 18633–18636.
[27] J.P. Conway, M. Kinter, Dual role of peroxiredoxin I in macrophage-derived foam cells, J. Biol. Chem. 281 (2006) 27991–28001.
[28] J.B. Seong, B. Kim, S. Kim, M.H. Kim, Y.H. Park, Y. Lee, et al., Macrophage peroxiredoxin 5 deficiency promotes lung cancer progression via ROS-dependent M2-like polarization, Free Radic. Biol. Med. 176 (2021) 322–334.
[29] M. Pirson, B. Knoops, Expression of peroxiredoxins and thioredoxins in the mouse spinal cord during embryonic development, J. Comp. Neurol. 523 (2015) 2599–2617.
[30] E. Dupuy, S.E. Van der Verren, J. Lin, M.A. Wilson, A.V. Dachsbeck, F. Viela, et al., A molecular device for the redox quality control of GroEL/ES substrates, Cell 186 (2023) 1039–1049, e17.
[31] Z.L. Chen, J.M. Meng, Y. Cao, J.L. Yin, R.Q. Fang, S.B. Fan, et al., A high-speed search engine pLink 2 with systematic evaluation for proteome-scale identification of cross-linked peptides, Nat. Commun. 10 (2019) 3404.
[32] E. Zito, PRDX4, an endoplasmic reticulum-localized peroxiredoxin at the crossroads between enzymatic oxidative protein folding and nonenzymatic protein oxidation, Antioxid. Redox Signal. 18 (2013) 1666–1674.
[33] H.I. Choi, K.J. Chung, H.Y. Yang, L. Ren, S. Sohn, P.R. Kim, et al., Peroxiredoxin V selectively regulates IL-6 production by modulating the Jak2-Stat5 pathway, Free Radic. Biol. Med. 65 (2013) 270–279.
[34] L. Chen, S. Wang, Y. Wang, W. Zhang, K. Ma, C. Hu, et al., IL-6 influences the polarization of macrophages and the formation and growth of colorectal tumor, Oncotarget 9 (2018) 17443–17454.
[35] Y.J. Lee, Knockout mouse models for peroxiredoxins, Antioxidants 9 (2020), https://doi.org/10.3390/antiox9020182.
[36] T. Ishii, K. Itoh, S. Takahashi, H. Sato, T. Yanagawa, Y. Katoh, et al., Transcription factor Nrf2 coordinately regulates a group of oxidative stress-inducible genes in macrophages, J. Biol. Chem. 275 (2000) 16023–16029.
[37] O. Liska, B. Bohar, A. Hidas, T. Korcsmaros, B. Papp, D. Fazekas, et al., TFLink: an integrated gateway to access transcription factor-target gene interactions for multiple species, Database 2022 (2022) baac083.
[38] C.C. Winterbourn, Biological production, detection, and fate of hydrogen peroxide, Antioxid. Redox Signal. 29 (2018) 541–551.
[39] Y. Ogura, Catalase activity at high concentration of hydrogen peroxide, Arch. Biochem. Biophys. 57 (1955) 288–300.
[40] J. Dalla Rizza, L.M. Randall, J. Santos, G. Ferrer-Sueta, A. Denicola, Differential parameters between cytosolic 2-Cys peroxiredoxins, PRDX1 and PRDX2, Protein Sci. 28 (2019) 191–201.
[41] T. Suzuki, A. Muramatsu, R. Saito, T. Iso, T. Shibata, K. Kuwata, et al., Molecular mechanism of cellular oxidative stress sensing by Keap1, Cell Rep. 28 (2019) 746–758, e4.
[42] B.C. Dickinson, D. Srikun, C.J. Chang, Mitochondrial-targeted fluorescent probes for reactive oxygen species, Curr. Opin. Chem. Biol. 14 (2010) 50–56.
[43] O. Lyublinskaya, F. Antunes, Measuring intracellular concentration of hydrogen peroxide with the use of genetically encoded H(2)O(2) biosensor HyPer, Redox Biol. 24 (2019), 101200.
[44] B.K. Huang, H.D. Sikes, Quantifying intracellular hydrogen peroxide perturbations in terms of concentration, Redox Biol. 2 (2014) 955–962.
[45] Z.A. Wood, L.B. Poole, P.A. Karplus, Peroxiredoxin evolution and the regulation of hydrogen peroxide signaling, Science 300 (2003) 650–653.
[46] T.F. Langford, B.K. Huang, J.B. Lim, S.J. Moon, H.D. Sikes, Monitoring the action of redox-directed cancer therapeutics using a human peroxiredoxin-2-based probe, Nat. Commun. 9 (2018) 3145.
[47] Y.S. Bae, J.H. Lee, S.H. Choi, S. Kim, F. Almazan, J.L. Witztum, et al., Macrophages generate reactive oxygen species in response to minimally oxidized low-density lipoprotein: toll-like receptor 4- and spleen tyrosine kinase-dependent activation of NADPH oxidase 2, Circ. Res. 104 (2009) 210–218, 21p following 8.
[48] M. Canton, R. Sanchez-Rodriguez, I. Spera, F.C. Venegas, M. Favia, A. Viola, et al., Reactive oxygen species in macrophages: sources and targets, Front. Immunol. 12 (2021), 734229.
[49] A.P. West, I.E. Brodsky, C. Rahner, D.K. Woo, H. Erdjument-Bromage, P. Tempst, et al., TLR signaling augments macrophage bactericidal activity through mitochondrial ROS, Nature 472 (2011) 476–480.
[50] A. Haschemi, P. Kosma, L. Gille, C.R. Evans, C.F. Burant, P. Starkl, et al., The sedoheptulose kinase CARKL directs macrophage polarization through control of glucose metabolism, Cell Metab. 15 (2012) 813–826.
[51] S. Gromer, L.D. Arscott, C.H. Williams Jr., R.H. Schirmer, K Becker, Human placenta thioredoxin reductase. Isolation of the selenoenzyme, steady state kinetics, and inhibition by therapeutic gold compounds, J. Biol. Chem. 273 (1998) 20096–20101.
[52] D. Ezerina, Y. Takano, K. Hanaoka, Y. Urano, T.P. Dick, N-acetyl cysteine functions as a fast-acting antioxidant by triggering intracellular H(2)S and sulfane sulfur production, Cell Chem. Biol. 25 (2018) 447–459, e4.
[53] E. Doka, T. Ida, M. Dagnell, Y. Abiko, N.C. Luong, N. Balog, et al., Control of protein function through oxidation and reduction of persulfidated states, Sci. Adv. 6 (2020) eaax8358.
[54] Q. Tian, S.B. Stepaniants, M. Mao, L. Weng, M.C. Feetham, M.J. Doyle, et al., Integrated genomic and proteomic analyses of gene expression in Mammalian cells, Mol. Cell. Proteom. 3 (2004) 960–969.
[55] B. Cox, T. Kislinger, A. Emili, Integrating gene and protein expression data: pattern analysis and profile mining, Methods 35 (2005) 303–314.
[56] M.S. Alam, Proximity Ligation Assay (PLA), Curr. Protoc. Immunol. 123 (2018) e58.
[57] H. Ichijo, E. Nishida, K. Irie, P. ten Dijke, M. Saitoh, T. Moriguchi, et al., Induction of apoptosis by ASK1, a mammalian MAPKKK that activates SAPK/JNK and p38 signaling pathways, Science 275 (1997) 90–94.
[58] D.J. Wadleigh, H.R. Herschman, Transcriptional regulation of the cyclooxygenase-2 gene by diverse ligands in murine osteoblasts, Biochem. Biophys. Res. Commun. 264 (1999) 865–870.
[59] N. Hannemann, J. Jordan, S. Paul, S. Reid, H.W. Baenkler, S. Sonnewald, et al., The AP-1 transcription factor c-jun promotes arthritis by regulating cyclooxygenase-2 and arginase-1 expression in macrophages, J. Immunol. 198 (2017) 3605–3614.
[60] R.K. Mishra, H.R. Potteti, C.R. Tamatam, I. Elangovan, S.P. Reddy, c-Jun is required for nuclear factor-kappaB-dependent, LPS-stimulated Fos-related Antigen-1 transcription in alveolar macrophages, Am. J. Respir. Cell Mol. Biol. 55 (2016) 667–674.
[61] J. Yu, Y. Wang, F. Yan, P. Zhang, H. Li, H. Zhao, et al., Noncanonical NF-kappaB activation mediates STAT3-stimulated IDO upregulation in myeloid-derived suppressor cells in breast cancer, J. Immunol. 193 (2014) 2574–2586.
[62] Y. Mochida, K. Takeda, M. Saitoh, H. Nishitoh, T. Amagasa, J. Ninomiya-Tsuji, et al., ASK1 inhibits interleukin-1-induced NF-kappa B activity through disruption of TRAF6-TAK1 interaction, J. Biol. Chem. 275 (2000) 32747–32752.
[63] J. Czupryna, A. Tsourkas, Xanthine oxidase-generated hydrogen peroxide is a consequence, not a mediator of cell death, FEBS J. 279 (2012) 844–855.
[64] A. Jezierska-Drutel, S. Attaran, B.L. Hopkins, J.J. Skoko, S.A. Rosenzweig, C. A. Neumann, The peroxidase PRDX1 inhibits the activated phenotype in mammary fibroblasts through regulating c-Jun N-terminal kinases, BMC Cancer 19 (2019) 812.
[65] T. Luo, J.M. Pueyo, K. Wahni, C. Yvanoff, T. Lazar, S. Pyr Dit Ruys, et al., Thiol-disulphide independent in-cell trapping for the identification of peroxiredoxin 2 interactors, Redox Biol. 46 (2021), 102066.
[66] F. Billia, L. Hauck, D. Grothe, F. Konecny, V. Rao, R.H. Kim, et al., Parkinson-susceptibility gene DJ-1/PARK7 protects the murine heart from oxidative damage in vivo, Proc. Natl. Acad. Sci. U. S. A. 110 (2013) 6085–6090.
[67] M. Capello, S. Ferri-Borgogno, C. Riganti, M.S. Chattaragada, M. Principe, C. Roux, et al., Targeting the Warburg effect in cancer cells through ENO1 knockdown rescues oxidative phosphorylation and induces growth arrest, Oncotarget 7 (2016) 5598–5612.
[68] R. Harjumaki, C.S. Pridgeon, M. Ingelman-Sundberg, CYP2E1 in alcoholic and non-alcoholic liver injury. Roles of ROS, reactive intermediates and lipid overload, Int. J. Mol. Sci. 22 (2021).
[69] A.K. Jha, S.C. Huang, A. Sergushichev, V. Lampropoulou, Y. Ivanova, E. Loginicheva, et al., Network integration of parallel metabolic and transcriptional data reveals metabolic modules that regulate macrophage polarization, Immunity 42 (2015) 419–430.
[70] S. Bonelli, X. Geeraerts, E. Bolli, J. Keirsse, M. Kiss, A.R. Pombo Antunes, et al., Beyond the M-CSF receptor - novel therapeutic targets in tumor-associated macrophages, FEBS J. 285 (2018) 777–787.
[71] J.M. Jaynes, R. Sable, M. Ronzetti, W. Bautista, Z. Knotts, A. Abisoye-Ogunniyan, et al., Mannose receptor (CD206) activation in tumor-associated macrophages enhances adaptive and innate antitumor immune responses, Sci. Transl. Med. 12 (2020), https://doi.org/10.1126/scitranslmed.aax6337.
[72] S.Y. Cheon, E.J. Kim, J.M. Kim, E.H. Kam, B.W. Ko, B.N. Koo, Regulation of microglia and macrophage polarization via apoptosis signal-regulating Kinase 1 silencing after ischemic/hypoxic injury, Front. Mol. Neurosci. 10 (2017), https://doi.org/10.3389/fnmol.2017.00261.
[73] M.M. Leblond, E.A. Peres, C. Helaine, A.N. Gerault, D. Moulin, C. Anfray, et al., M2 macrophages are more resistant than M1 macrophages following radiation therapy in the context of glioblastoma, Oncotarget 8 (2017) 72597–72612.
[74] T.A. Zykova, F. Zhu, T.I. Vakorina, J. Zhang, L.A. Higgins, D.V. Urusova, et al., T-LAK cell-originated protein kinase (TOPK) phosphorylation of Prx1 at Ser-32 prevents UVB-induced apoptosis in RPMI7951 melanoma cells through the regulation of Prx1 peroxidase activity, J. Biol. Chem. 285 (2010) 29138–29146.